

Direct Numerical Simulations of Fundamental Turbulent Flows with the World's Largest Number of Grid-points and Application to Modeling of Engineering Turbulent Flows

Project Representative

Takashi Ishihara Graduate School of Engineering, Nagoya University

Authors

Takashi Ishihara Graduate School of Engineering, Nagoya University

Yukio Kaneda Aichi Institute of Technology

Kaoru Iwamoto Mechanical Systems Engineering, Tokyo University of Agriculture and Technology

Tetsuro Tamura Interdisciplinary Graduate School of Science and Engineering, Tokyo Institute of Technology

Yasuo Kawaguchi Department of Mechanical Engineering, Tokyo University of Science

Takahiro Tsukahara Department of Mechanical Engineering, Tokyo University of Science

High-resolution direct numerical simulations (DNS) of canonical turbulence were performed on the Earth Simulator 2. They include (i) high-Reynolds-number turbulent channel flows with the friction Reynolds number up to 5120 and (ii) turbulent boundary layers on sinusoidal wavy walls. They provide us with invaluable detailed information on the related turbulence phenomena. The analyses of the DNS data show the following. (1) The spectrum of the cross correlation between the streamwise and wall-normal fluctuating velocity components in the log-law region agrees well with the corresponding spectrum obtained in the inertial sub-range of homogeneous shear turbulence. (2) In the TBL with a sinusoidal wavy wall, the dissimilarity between momentum and mass transfers appears. We also performed the turbulence simulations for environmental and industrial applications; (iii) Large-scale LES of turbulent flows for strong wind disaster mitigation and (iv) DNS of turbulent flow of non-Newtonian surfactant solution passing complicated geometry. The results of these simulations show the following. (3) By imposing the turbulent wind with specific characteristics, the LES can be used for the estimation of the wind-resistant performance of the specified building that is located within many buildings arrayed densely. (4) In a channel flow with bluff bodies of finite plates for a viscoelastic fluid, the frictional-drag reduction occurs just behind the bluff body, because the Kelvin-Helmholtz eddies are dampened significantly.

Keywords: High-resolution DNS, turbulent channel flow, turbulent boundary layer, rough wall, LES, urban turbulent boundary layer, non-Newtonian fluid, drag reduction

1. Direct numerical simulations of fundamental turbulent flows

1.1 High resolution DNS of turbulent channel flow

To investigate the small-scale statistics in wall-bounded high-Reynolds-number turbulence, we performed a series of direct numerical simulations (DNS) of turbulent channel flows (TCF) with the friction Reynolds number Re_τ up to 5120. In the DNS, we solved the incompressible Navier-Stokes (NS) equations using the Fourier-spectral method in the streamwise(x) and spanwise(z) directions and the Chebyshev-tau method in the wall-normal(y) direction. The computational domain is $\pi h \times 2h \times \pi h/2$ (small box) and $2\pi h \times 2h \times \pi h$ (larger box) for the DNS with Re_τ up to 2560 and is $\pi h \times 2h \times \pi h/2$ (small box) for the DNS with $Re_\tau = 5120$. In the fiscal year of 2012, we generated a

TCF database with $Re_\tau = 5120$ using the TCF code that achieves a performance of 6.1 Tflops (11.7% of the peak performance) on 64 nodes of ES2. The TCF with the largest value of Re_τ was simulated until time t as large as 14 wash-out-times, to study the small-scale statistics at a statistically steady state of the turbulence. Table 1 gives a summary of our DNS database.

Data analysis showed that the small-scale statistics in TCF are insensitive to whether the box size is small (S) or large (L), at least in our cases. The DNS with high values of Re_τ exhibit a range where the mean stream-wise velocity U fits well to the log-law and the energy dissipation rate is nearly inversely proportional to the distance from the wall. The width of the range (in the wall unit normalized by u_τ and h) increases with the values of Re_τ . In Case 5S, the maximum Taylor microscale

Table 1 Parameters used in the series of the DNS of TCF. h is the channel half width; L_x, L_z , fundamental periodic lengths in the streamwise(x) and spanwise(y) directions, respectively; N_x, N_y, N_z , the number of grid points in the x, y, z -directions; Δx^+ and Δz^+ , the mesh size (normalized by u_τ and h) in the x, z -directions, and Δy_c^+ is the wall-normal mesh size at the channel center.

	Re_τ	L_x/h	L_z/h	$N_x \times N_y \times N_z$	Δx^+	Δy_c^+	Δz^+
Case 1S	320	π	$\pi/2$	$128 \times 192 \times 128$	7.9	7.9	3.9
Case 1L	320	2π	π	$256 \times 192 \times 256$	7.9	7.9	3.9
Case 2S	640	π	$\pi/2$	$256 \times 384 \times 256$	7.9	7.9	3.9
Case 2L	640	2π	π	$512 \times 384 \times 512$	7.9	7.9	3.9
Case 3S	1280	π	$\pi/2$	$512 \times 768 \times 512$	7.9	7.9	3.9
Case 3L	1280	2π	π	$1024 \times 768 \times 1024$	7.9	7.9	3.9
Case 4S	2560	π	$\pi/2$	$1024 \times 1536 \times 1024$	7.9	7.9	3.9
Case 4L	2560	2π	π	$2048 \times 1536 \times 2048$	7.9	7.9	3.9
Case 5S	5120	π	$\pi/2$	$2048 \times 1536 \times 2048$	7.9	15.9	3.9

Reynolds number $R_\lambda=370$ was attained at $y^+ \sim 1200$ in the log-law range. In the range, the spectrum $E_{12}(k_1)$ of the cross correlation between the streamwise and wall-normal fluctuating velocity components fits well to the $-7/3$ power law in the inertial sub-range, where k_1 is the wavenumber in the streamwise direction. Its pre-factor was shown to be in good agreement with laboratory experiments of turbulent boundary layer by Saddoughi et al [1] and Tsuji [2], and DNS of homogeneous turbulent shear flow by Ishihara et al [3].

2. DNS of turbulent boundary layer on rough walls

Turbulent boundary layer flow over a rough wall is one of canonical flows, while is important in fundamental turbulent researches, practical engineering applications and environmental problems. The DNS code optimized for ES2 is employed to investigate the effect of a sinusoidal wavy wall surface which is a simple model of the roughness. The amplitude of the sinusoidal wavy wall, a , is kept constant in wall units, whereas different wavelengths λ are investigated for $\lambda / 2a = 12.5, 15, 22.5$ and 45 .

For the spatially developing boundary layer flow over the sinusoidal wavy wall, we provide a driver and a main computational domains as shown in Fig. 1. The driver part provides an inflow condition of the main part, where the recycle method [4] is used. The main part has the sinusoidal wavy wall. The parallel and vectorization efficiencies of the present DNS code are 98.43% and 99.50%, respectively. In this year, we focus on the dissimilarity between the momentum and the mass

transfers.

Figure 2 visualizes the distribution of the wall shear stress and the Sherwood number. The Sherwood number is the dimensionless number of the mass transfer. The high wall shear stress appears on the top of the wavy wall. On the other hand, the Sherwood number is high not only on the top, but also in the valley of the wavy wall. This indicates that the dissimilarity between the momentum and the mass transfers appears.

3. Large-scale LES of turbulent flows for strong wind disaster mitigation

For the mitigation of strong wind disaster, large scale LES (Large eddy simulation) has been performed using the actual urban model. The actual shape of building and structure is individually reproduced in the broad area of a city. The wind characteristics at high altitude above a city are spatially and temporally analyzed and its relation with the surface roughness is elucidated. By imposing the turbulent wind with specific characteristics, LES has been carried out for the estimation of the wind-resistant performance of the specified building which is located within many buildings arrayed densely. Details of wind forces acting on the surface of building were discussed with indicating the occurrence of the peak pressure at local area by the surrounding building or some special geometry of building itself.

Figure 3 illustrates the numerical model for LES of the wind flows among the tall buildings in the actual city. The target building for the estimation of wind pressures is surrounded by

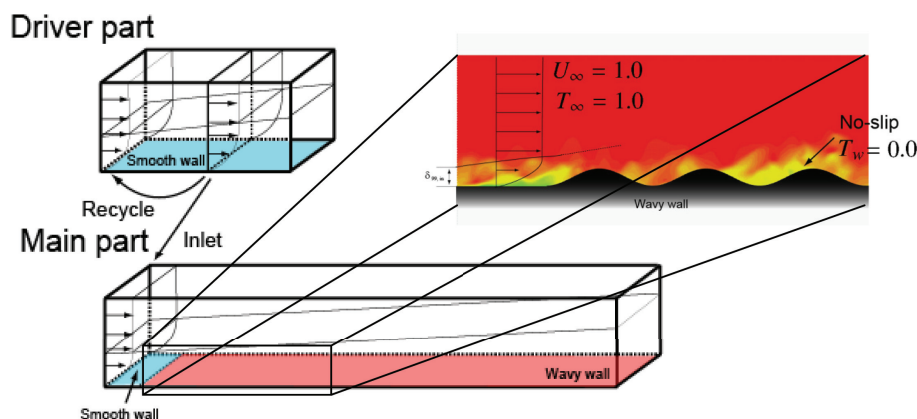


Fig. 1 Computational domains for turbulent boundary layer flow and the sinusoidal wavy wall.

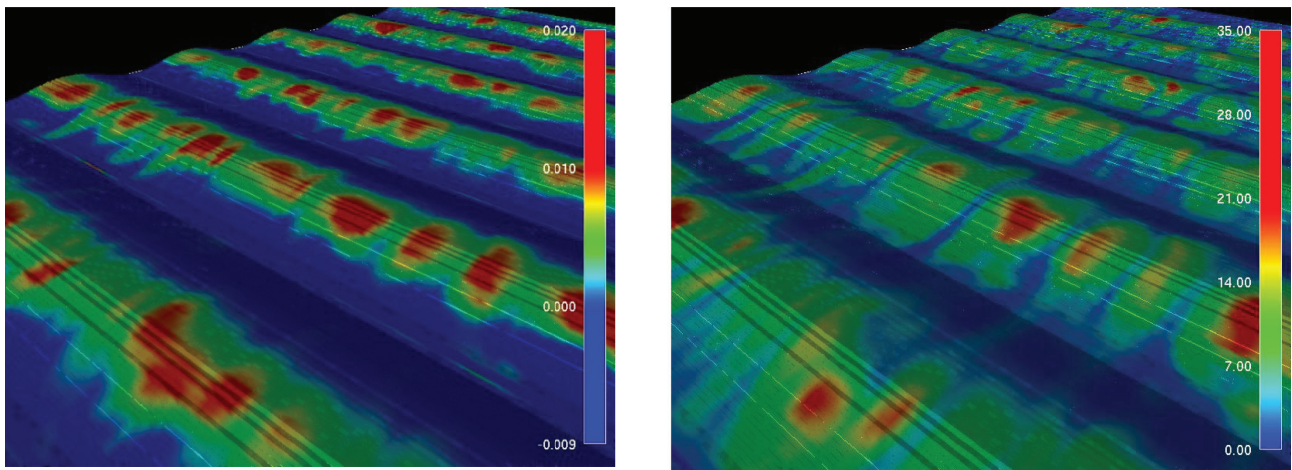


Fig. 2 Distribution of the wall shear stress (left) and the Sherwood number (right) on the wavy wall surface ($\lambda / 2a = 12.5$).

the other many tall buildings. For investigating details of the complex flows among many buildings and their wakes with smaller scale, the shape of each building is directly reproduced. Figure 4 shows the pressure distributions around the tall building surrounded by other tall buildings at wind direction from south. Some special characteristics with bias of the spatial distribution of pressure are actually recognized as we can find in the experimental data. This LES model is also validated by comparing with field measurement data of wind-induced oscillations. Furthermore, we investigate details of a local flow patterns among buildings (Fig. 5) and provide a dominant role of the shape and the direction of the specified building to determine the wind forces in view of the mitigation of strong wind disaster.

Recent architectural buildings have a variety of shapes based on unique designer concepts, and the curved surfaces are frequently used for building wall. Here, as a typical and a fundamental case in such buildings, a circular cylinder is focused on. The flow characteristics around a circular cylinder in realistic high Reynolds number region are investigated by use of the LES model. As a result, the present LES model succeeded in simulating the aerodynamic characteristics and flow characteristics at the critical Reynolds numbers (Figs. 6 and 7). The present computations clarified the characteristics of the local lift coefficients associated with the three-dimensionalities of the wake structures in the span-wise direction at the critical Reynolds numbers.

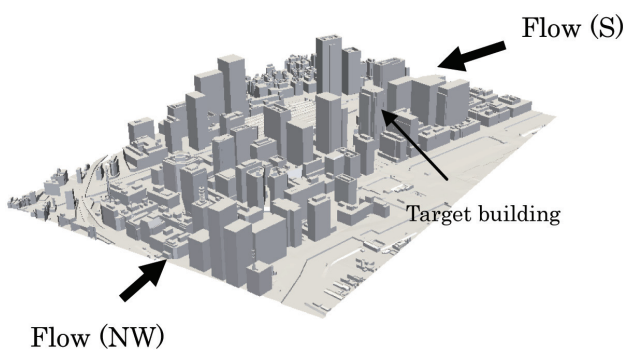


Fig. 3 LES model of wind flows in the city.

4. DNS of turbulent heat transfer of non-Newtonian surfactant solution passing complicated geometry

Turbulent drag reduction by surfactant additives in liquid fluid flow is of importance and profitable for saving energy in the fluid transportation, such as oil-pipeline circuits or district heating and cooling (DHC) recirculation systems [5]. The surfactant solutions that give rise to the drag reduction reveal viscoelasticity (and become non-Newtonian). The viscoelastic-fluid flow through complex geometries has attracted fundamental scientific interest and related to numerous practical applications, such as flows associated with chemical,

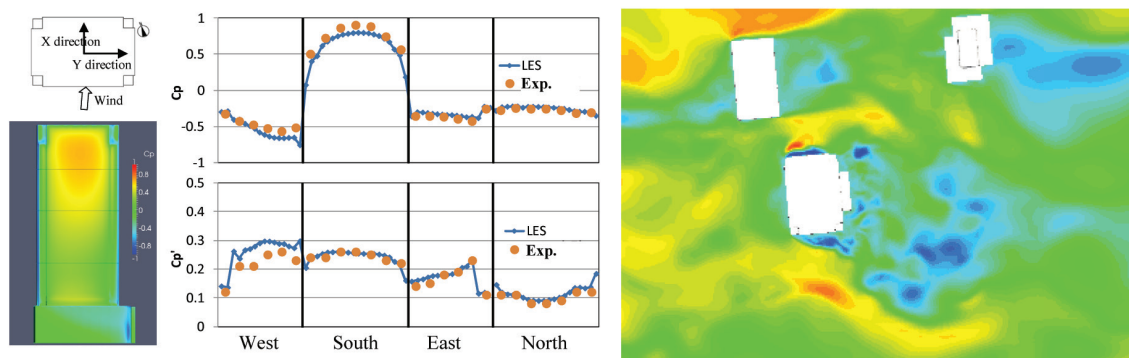


Fig. 4 Pressure distributions and flow patterns around the tall building (South wind).

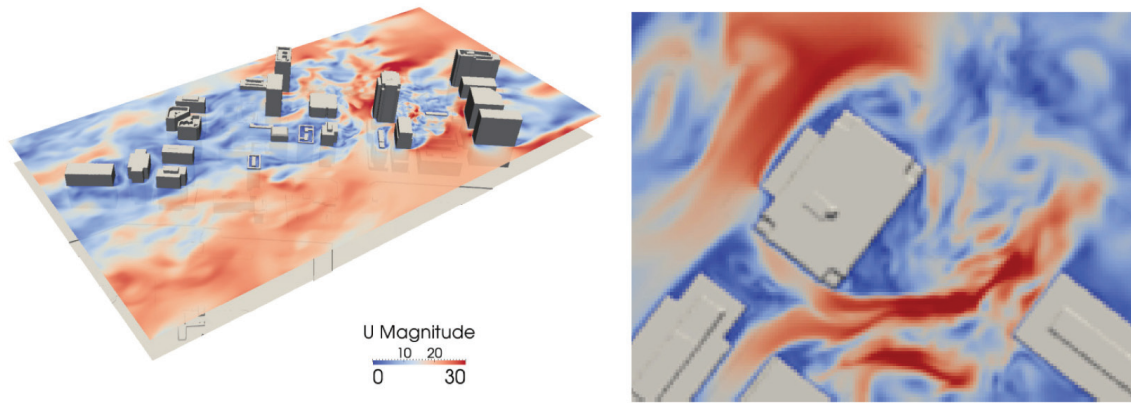


Fig. 5 Flow patterns around the tall building (Northwest wind).

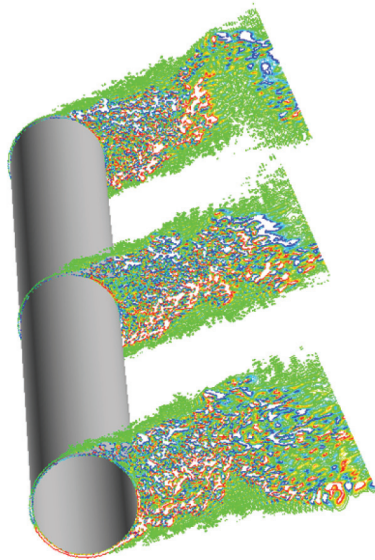


Fig. 6 Wake structures of a circular cylinder ($Re=2 \times 10^5$).

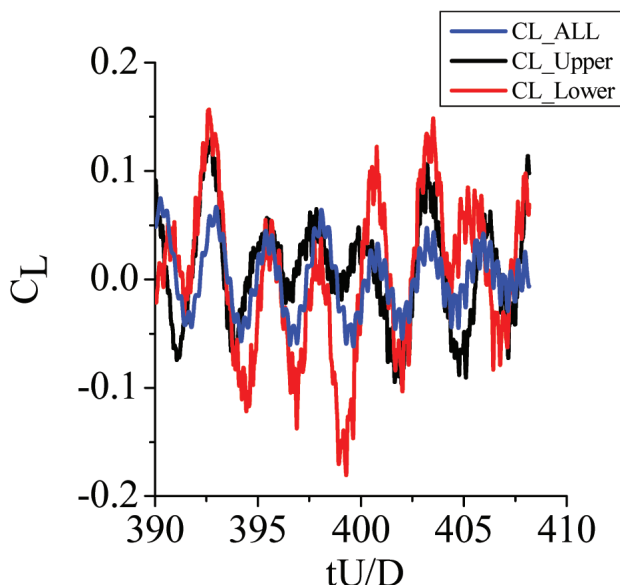


Fig. 7 Time histories of lift coefficients of a circular cylinder ($Re=2 \times 10^5$).

pharmaceutical, food processing, and biomedical engineering, where the analysis and designing for their pipe-flow systems are more difficult than for its Newtonian counterpart. However, complex features and behavior of the turbulent viscoelastic flow through complicated geometries are still unclear. The present study is aimed to address this issue.

Based on Giesekus' viscoelastic-fluid model [6], DNS of turbulent flow of a viscoelastic fluid passing finite planes has been carried out. The computational methods we used here were basically same with those in Tsukahara et al. [7]. The goal of this work is to better understand the fluid-dynamics characteristics of the viscoelastic turbulent flow behind bluff bodies. Major differences between the present study and published works on smooth channels are related to the streamwise variation of the flow state and the existence of secondary-flow structures in the form of large-scale longitudinal vortices. Therefore, the instantaneous vortex structures and the relevant momentum transfer and frictional-drag reduction within the strong shear layer just downstream of the orifice should be explored.

Figure 8 shows instantaneous flow field both of the Newtonian fluid and the viscoelastic fluid, where vortex structures are visualized by the second invariant of the deformation tensor. In the Newtonian flow, many vortices are induced just behind the plate and they decay gradually as propagating downstream. The viscoelastic flow reveal less vortices and, in regions far from the plate, relatively large-scale eddies are visible. Some vortices that elongate in the streamwise direction (i.e., longitudinal vortices) appear dominantly. If focusing on the strong shear layer just downstream of the plate edge, we can observe the spanwise primary Kelvin-Helmholtz (K-H) vortices in Fig. 8(a), but almost absent in Fig. 8(b) so that small-scale eddies do not occur. This is consistent with our previous study on the orifice flow [7], which reported the K-H vortices decayed quickly downstream of the orifice in viscoelastic fluid. Figure 9 shows the reduction rate of the streamwise drag force, and Fig. 10 shows the local skin friction coefficient at either $z^* = z/\delta = 0$ (plate-free region) or 3.2 (the plate center). From those results, we may draw conclusions

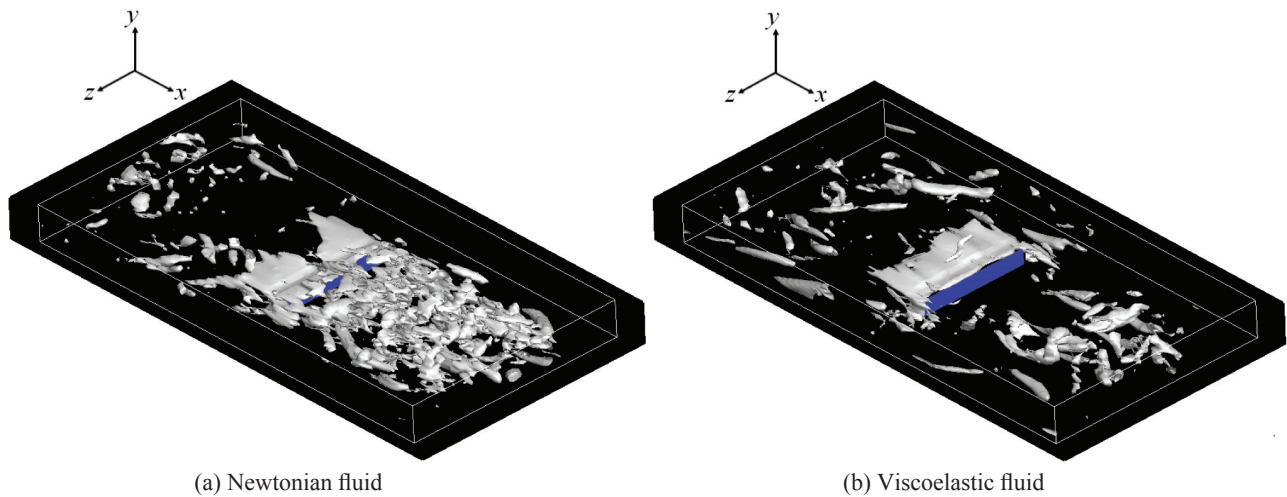


Fig. 8 Instantaneous vortex structures around the rib on the bottom wall: iso-surfaces of the second invariant of the deformation tensor. The main stream direction is from top-left to bottom-right.

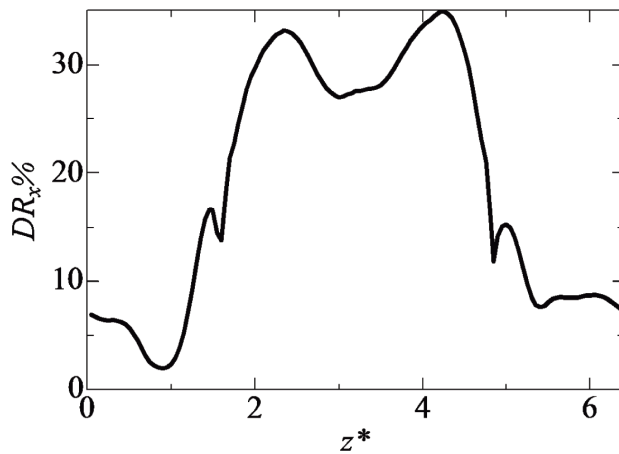


Fig. 9 Spanwise distribution of the percent drag reduction averaged in the streamwise direction. The finite plate is spanned in $z^* = 1.6-3.2$.

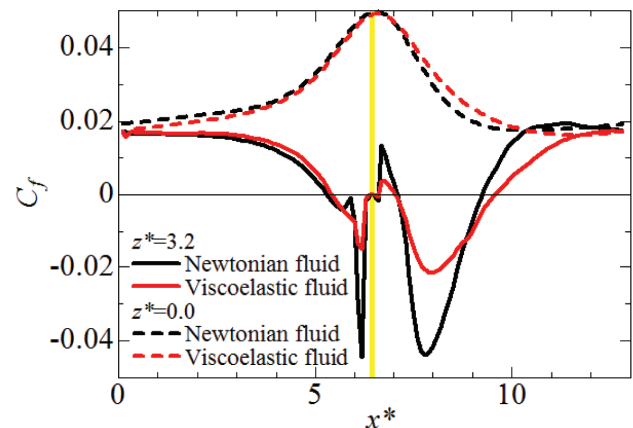


Fig. 10 Streamwise distribution of the local skin friction coefficient. The finite plate is located at $x^* = 6.4$.

that a large drag reduction occurs at the rib location and that a significant reduction occurs in some extent behind the ribs, where wall-normal and spanwise vortices are suppressed.

References

- [1] S. G. Saddoughi and S. V. Veeravalli, "Local isotropy in turbulent boundary layers at high Reynolds number," *J. Fluid Mech.*, 268, 333-372 (1994).
- [2] Y. Tsuji, "Large-scale anisotropy effect on small-scale statistics over rough wall turbulent boundary layers," *Phys. Fluids*, 15(12), 3816-3828 (2003).
- [3] T. Ishihara, K. Yoshida, and Y. Kaneda, "Anisotropic velocity correlation spectrum at small scales in a homogeneous turbulent shear flow," *Phys. Rev. Lett.*, 88(15), 154501 (2002).
- [4] T. S. Lund, X. Wu, and K. D. Squires, "Generation of turbulent inflow data for spatially-developing boundary layer simulations," *J. Comput. Phys.*, 140 (2), 233-258, (1998).
- [5] H. Takeuchi, "Demonstration test of energy conservation of central air conditioning system at the Sapporo city office building—Reduction of pump power by flow drag reduction using surfactant," *Synthesiology—English edition*, vol. 4, 136-143, (2012).
- [6] H. Giesekus, "A simple constitutive equation for polymer fluids based on the concept of deformation-dependent tensorial mobility," *Journal of Non-Newtonian Fluid Mechanics*, vol. 11, 69-109, (1982).
- [7] T. Tsukahara, T. Kawase, and Y. Kawaguchi, "DNS of viscoelastic turbulent channel flow with rectangular orifice at low Reynolds number," *International Journal of Heat and Fluid Flow*, vol. 32, 529-538, (2011).

乱流の世界最大規模直接数値計算とモデリングによる応用計算

プロジェクト責任者

石原 卓 名古屋大学 大学院工学研究科

著者

石原 卓 名古屋大学 大学院工学研究科

金田 行雄 愛知工業大学

岩本 薫 東京農工大学 工学府

田村 哲郎 東京工業大学 大学院総合理工学研究科

川口 靖夫 東京理科大学 理工学部

塚原 隆裕 東京理科大学 理工学部

地球シミュレータ (ES2) を用いて、(i) 高レイノルズ数 (壁摩擦速度に基づくレイノルズ数 5120) の平行平板間乱流、(ii) 正弦波状壁面上の乱流境界層を含む、カノニカルな問題の大規模直接数値シミュレーション (DNS) を実施した。これらの DNS は、関連する乱流現象に対して詳細で有益な情報を与えるものである。これらの DNS で得られたデータを解析することにより (1) 高レイノルズ数壁乱流の対数則領域で得られる流れ方向の速度揺らぎと壁垂直方向の速度揺らぎの相関スペクトルが単純剪断乱流の慣性小領域で得られるスペクトルとよく一致すること、および、(2) 正弦波状の壁における壁乱流の壁面摩擦と汚染物質拡散の非相似性を示すことを見出した。また、我々は環境や工学的な応用問題に対する乱流数値計算として、(iii) 実際の都市を対象とした、環境・防災問題の低減化をめざした高解像度大規模乱流のラージ・エディ・シミュレーション (LES)、(iv) リブ列を有する複雑流路内乱流の DNS 実施と粘弾性流体の熱流動特性評価を実施した。これらにより、(3) LES において都市上空における強い風の時空間構造の特性を有する流れを用いることで、都市部における建物群の中にある当該建築物の耐風性能評価が可能であること、および、(4) リブ列を有する平行平板間の粘弾性流体乱流においては、同じ境界条件におけるニュートン流体の流れと異なり、リブ後方でケルビン・ヘルムホルツ不安定によって発生する渦が著しく抑制され、その結果として抵抗低減が起きることが判明した。

キーワード: 大規模直接数値計算, 平行二平板間乱流, 乱流境界層, 粗面, LES, 都市型乱流境界層, 界面活性剤, 抵抗低減